Human Molecular Genetics, 2011, Vol. 20, No. 21 ***4143–4154***
doi:10.1093/hmg/ddr338
Advance Access published on August 5, 2011

Pyrimethamine inhibits adult polycystic kidney disease by modulating STAT signaling pathways

Ayumi Takakura[1,*], Erik A. Nelson[2], Nadeem Haque[1], Benjamin D. Humphreys[1], Kambiz Zandi-Nejad[1], David A. Frank[2] and Jing Zhou[1,*]

[1]Renal Division, Department of Medicine, Brigham and Women's Hospital and [2]Department of Medical Oncology, Dana-Farber Cancer Institute, and Harvard Medical School, Boston, MA 02115, USA

Received April 14, 2011; Revised and Accepted August 1, 2011

Autosomal dominant polycystic kidney disease (ADPKD) is a commonly inherited disorder mostly caused by mutations in *PKD1*, encoding polycystin-1 (PC1). The disease is characterized by development and growth of epithelium-lined cyst in both kidneys, often leading to renal failure. There is no specific treatment for this disease. Here, we report a sustained activation of the transcription factor signal transducer and activator of transcription 3 (STAT3) in ischemic injured and uninjured *Pkd1* knockout polycystic kidneys and in human ADPKD kidneys. Through a chemical library screen, we identified the anti-parasitic compound pyrimethamine as an inhibitor of STAT3 function. Treatment with pyrimethamine decreases cell proliferation in human ADPKD cells and blocks renal cyst formation in an adult and a neonatal PKD mouse model. Moreover, we demonstrated that a specific STAT3 inhibitor, S3I-201, reduces cyst formation and growth in a neonatal PKD mouse model. Our results suggest that PC1 acts as a negative regulator of STAT3 and that blocking STAT3 signaling with pyrimethamine or similar drugs may be an attractive therapy for human ADPKD.

INTRODUCTION

Autosomal dominant polycystic kidney disease (ADPKD) is a commonly inherited disorder characterized by increased proliferation of epithelial cells and gradual replacement of normal renal parenchyma by fluid-filled cysts with ultimate loss of renal function. About half of the patients require organ transplantation (1,2). Mutations in *PKD1*, which encodes polycystin-1 (PC1), are responsible for 85% of ADPKD cases.

We and other groups have previously generated *Pkd1* inducible knockout (IKO) mice and showed that *Pkd1* inactivation in the developing kidney results in rapid cyst formation (3–5), whereas loss of *Pkd1* in adult kidney induces only slow focal cyst formation. In contrast to the developing kidney, the adult kidney epithelia are terminally differentiated and proliferate at a very low rate. It is noteworthy that similar to kidney development, PC1 expression is high during late embryogenesis and the first 2 weeks after birth. Ischemia reperfusion injury (IRI), which reactivates a renal developmental program and triggers epithelial cell proliferation (6), causes massive cystic lesions in these mice (7). We therefore hypothesized that PC1 may act as a regulator of developmental signaling pathways and cell proliferation. Most studies on ADPKD orthologous models were performed on immature kidneys. Whether the molecular mechanisms underlying cyst formation in the mature kidney are the same as in the developing kidney is unknown.

The Janus kinase/signal transducer and activator of transcription (JAK/STAT) pathway is critical for developmental regulation, growth control and homeostasis in organs (8–12). Phosphorylation of STAT3 at tyrosine 705 occurs in response to a variety of cytokines and growth factors including interleukin-6 (IL-6), epidermal growth factor and hepatocyte growth factor (13,14). The expression of these cytokine and growth factors is associated with PKD progression (15–17). Interestingly, ciliary neurotrophic factor-induced phosphorylation at serine 727 of STAT3 is reported to be mediated by the mTOR pathway (18), which is also up-regulated in both ADPKD kidneys (19) and ischemic injured rat kidneys (20). Constitutively activated STAT3 and the overexpression of its downstream target gene cyclin D1 are seen in many solid tumors including head and neck squamous cell carcinoma (21) and renal cell carcinoma (22,23). The relationship

*To whom correspondence should be addressed at: Harvard Institutes of Medicine, Room 520, 4 Blackfan Circle, Boston, Massachusetts 02115, USA. Tel: +617 525 5860; Email: zhou@rics.bwh.harvard.edu (J.Z.); Tel: +617 525 5867; Email: atakakura@rics.bwh.harvard.edu (A.T.)

between STAT3-mediated signaling pathway and ADPKD, however, is not clear. After this work was completed, Leonhard *et al*. (24) reported that curcumin treatment reduced the elevated STAT3 and S6 phosphorylation in iKsp-*Pkd1*^{del} mouse kidneys and delayed the onset of renal failure by 10 days in this mouse model. Curcumin, however, has a variety of effects beyond its inhibition of STAT3 activity. Whether STAT3 would be an effective drug target for the treatment of ADPKD remains unknown.

Here, we show that STAT3 is activated in mouse and human PKD1 disease. The anti-parasitic drug pyrimethamine and another compound STAT3 inhibitor, S3I-201, significantly inhibit the cyst formation and growth in adult onset PKD mouse model and neonatal PKD mouse model, respectively.

RESULTS

The activation of STAT3 is increased in mouse cystic kidney and human ADPKD kidney

We first looked at the activation of STAT3 in cystic kidneys of 1-week-old *Col2Cre*$^{+}$*Pkd1*$^{flox/flox}$ conditional knockout (CKO) mice (25), which is a rapid model for cystogenesis. These mice develop cysts around birth and die 12–14 days after birth due to severe polycystic kidney disease. In addition to a PKD phenotype, *Col2Cre*$^{+}$*Pkd1*CKO display a mild reduction in the cortical bone deposition and cranial base defects (25). As expected, the levels of tyrosine phosphorylated active STAT3 (pSTAT3) as well as total STAT3 protein significantly increased in cystic kidneys in PKD mouse model, compared with those in littermate control kidneys (Fig. 1A). To investigate the expression of STAT3-dependent transcription, we performed real-time reverse transcriptase–polymerase chain reaction (RT–PCR) of cyclin D1, cyclin D2, c-Myc and Bcl-X. Significantly increased steady-state transcript levels of these STAT3 target genes after normalization with β-actin are evident in these mouse cystic kidneys (Fig. 1B). In addition, STAT3 mRNA levels were also significantly increased. Since the *Col2Cre*$^{+}$-*Pkd1*$^{flox/flox}$ CKO mice die during post-natal development, we switched to the *Mx1Cre*$^{+}$*Pkd1* IKO mouse models for further experiments. The IKO mice survive much longer and more closely resemble human ADPKD. In addition to an increased pSTAT3 level, we also observed striking nuclear localization of pSTAT3 in a subset of cyst-lining epithelial cells from the *Mx1Cre*$^{+}$*Pkd1* IKO model (Fig. 1C). No pSTAT3 signal was found in the wild-type kidneys (Fig. 1C). IL-6 was previously found in renal cystic fluid from human ADPKD patients (16). We found ∼6-fold higher levels of IL-6 in *Pkd1* IKO cystic kidneys than their littermate control kidneys (Fig. 1D). To exclude the possibility that this up-regulation of STAT3 activation is unique to the PKD mouse models, we performed immunoblotting for pSTAT3 on human ADPKD and non-PKD kidneys. Consistent with our findings in mouse kidneys, increased pSTAT3 was also observed in human ADPKD kidneys (Fig. 1E). Moreover, we detected an increase in pSTAT3 in cyst-lining epithelial cells derived from a human ADPKD kidney when compared with cells from a normal (non-PKD) kidney (Fig. 1G). We also found pSTAT3 in the nuclei of relatively small cyst-lining epithelial cells in human ADPKD kidneys but not in non-PKD kidneys by immunostaining (Fig. 1F and Supplementary Material, Fig. S1A). Thus, STAT3 activation is up-regulated in both mouse cystic kidneys and human ADPKD kidney.

Identification of pyrimethamine as a STAT3 inhibitor through a mechanistic-based screen

Recently two human clinical trial studies have shown that mTOR inhibitors, sirolimus and everolimus, did not significantly benefit patients with ADPKD (26–28). Furthermore, inhibition of mTOR can have significant side effects (29). To discover clinically relevant drugs that would be safe in humans and potentially effective for the treatment of ADPKD, we focused on identifying small molecule inhibitors of STAT3 transcriptional activity. A cell-based functional assay was utilized (30), and compounds from the Prestwick collection, a library of 1120 small molecules biased toward bioactives and drugs known to be safe in humans, were interrogated for the ability to inhibit STAT3, while having little to no effect in a counter-screen of nuclear factor κ-light-chain-enhancer of activated B cells (NFκB)-dependent transcriptional activity. From this screen, the anti-parasitic compound pyrimethamine was identified. Over a broad range of concentrations, pyrimethamine inhibited STAT3-dependent reporter gene expression while having no effect on transcription driven by NFκB or the highly homologous transcription factor STAT5 (Fig. 2).

Pyrimethamine inhibits STAT3 tyrosine phosphorylation in a human ADPKD cell line

To determine whether pyrimethamine reduces STAT3 phosphorylation in human ADPKD epithelial cells, confluent ADPKD cells were cultured in the presence of pyrimethamine at a range of concentrations for 24 h and analyzed by western blotting. We found that pyrimethamine significantly decreased pSTAT3 in a dose-dependent manner and reduced the pSTAT3/STAT3 ratio by ∼33 or ∼72% (50 or 100 μM Py), without changing the total STAT3 level (Fig. 3A). In contrast, pyrimethamine only had a modest effect in non-PKD human epithelial cells [renal cortical tubular epithelia cell (RCTEC); Fig. 3B]. Along with the reduction in pSTAT3, the viability of pyrimethamine-treated ADPKD cells also decreased in a dose-dependent manner (Fig. 3C). To determine whether this decrease in viable cell number reflected decreased proliferation or increased apoptosis, we assessed cell proliferation by flow cytometry and apoptosis by DNA fragmentation assay. We found that there was a significant reduction in the G2/M phase and an increase in the S phase in pyrimethamine-treated ADPKD cells (Fig. 3D and Supplementary Material, Table S1), indicating that pyrimethamine induced an S-phase arrest. DNA ladder formation was evident in pyrimethamine-treated cells, indicating an increase in apoptosis (Fig. 3E). Thus, besides reducing pSTAT3 levels, pyrimethamine inhibits cell proliferation by blocking cell cycle progression and inducing programmed cell death in ADPKD cells. Importantly, pyrimethamine decreased the number of viable cells (Fig. 3F), the status of cell cycle (Fig. 3G) and DNA fragmentation (Fig. 3H) only at a high dose in normal RCTEC cells. These data suggest that

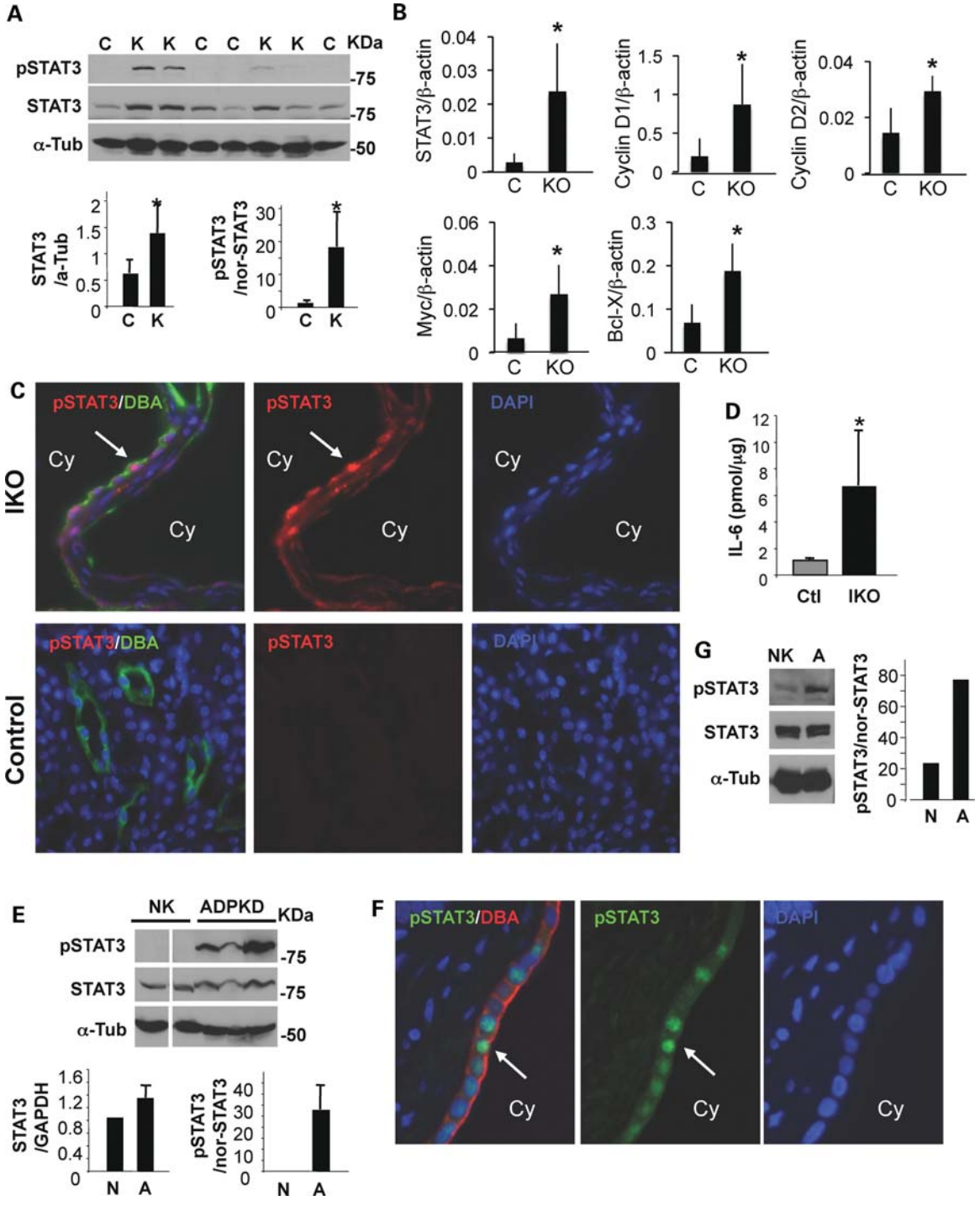

Figure 1. STAT3 is activated in mouse and human cystic kidneys. (**A**) The kidney lysates from four 1-week-old *Col2-Cre*$^{+}$*Pkd1* CKO (K) and four littermate control (C) mice were blotted with indicated antibodies. α-Tubulin was used as a loading control. STAT3 expression is normalized to α-tubulin ($^{*}P < 0.03$) and the ratio of pSTAT3/STAT3 is normalized to α-tubulin ($^{*}P < 0.007$). (**B**) Real-time RT–PCR was performed on cDNA from three 1-week-old Col2-Cre*Pkd1* CKO (KO) and three littermate control (C) kidneys. There were significantly increased expression of STAT3 ($P < 0.04$), c-Myc ($P < 0.04$), cyclin D1 ($P < 0.05$), cyclin D2 ($P < 0.03$) and bcl-X ($P < 0.03$) in CKO mice. (**C** and **F**) Representative immunostaining of kidneys from *Mx1Cre*$^{+}$*Pkd1* IKO and littermate control mice (**C**) or from ADPKD patients (**F**) with anti-pSTAT3 antibodies and DBA. Arrow points to STAT3 nuclear staining in cyst-lining epithelial cells. 'Cy' represents cyst lumen. (**D**) IL-6 production in kidney lysates was measured by enzyme-linked immunosorbent assay [6.69 ± 4.13 (IKO) versus 1.12 ± 0.09 (Ctl) pmol/μg, $n = 3$ mice per each genotype, $^{*}P < 0.04$]. (**E** and **G**) Western blot of pSTAT3 and total STAT3 in human kidney lysates from five unrelated female individuals (44–63-year-old) with ADPKD (ADPKD) or without ADPKD (NK) (**E**) and in renal epithelial cells from patients with non-PKD (N) and ADPKD (A) (**G**). α-Tubulin was used as a loading control. All data shown were expressed as the mean ± SD. The size of STAT3α, STAT3β and α-tubulin is 79, 86 and 55 kDa, respectively. The protein markers are indicated.

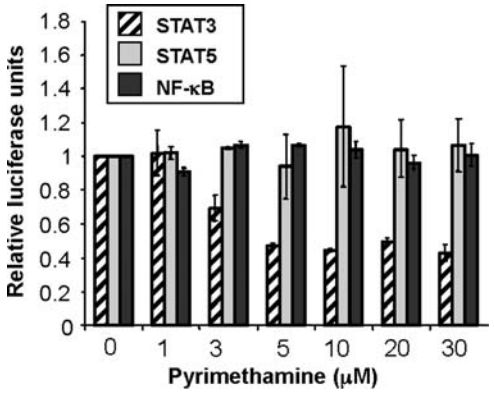

Figure 2. Pyrimethamine specifically inhibits STAT3-dependent reporter gene expression. Cells were pretreated with the indicated concentrations of pyrimethamine for 1 h prior to cytokine stimulation as described in Materials and methods.

pyrimethamine preferentially affects the ADPKD cells and is an attractive candidate for ADPKD treatment.

STAT3 is known to be activated by cytokine receptors (through phosphorylation by Jak family kinases) and growth factor receptors (13). To determine whether this increased STAT3 activation in ADPKD cells is mediated by an upstream Jak family member, the cells were treated with nifuroxazide, which inhibits Jak2 activity and in turn decreases STAT3 phosphorylation (30). Similar to pyrimethamine, nifuroxazide also reduced pSTAT3 in a dose-dependent manner, by ~40 or 84% (50 or 100 μM Nif; Fig. 3I). Furthermore, another well-characterized Jak2 inhibitor, Jak inhibitor 1, dramatically reduced pSTAT3 in ADPKD cells (Supplementary Material, Fig. S1B). Thus, activation of STAT3 in ADPKD cells is due to increased Jak2 activity. Since Jak2 also activates STAT1 in addition to STAT3, we immunoblotted pSTAT1 in pyrimethamine-treated ADPKD cells. Interestingly, pyrimethamine did not inhibit STAT1, but increased the pSTAT1/STAT1 ratio to ~2-fold (Fig. 3J). These data suggest that the inhibitory effect of pyrimethamine on STAT3 is not through Jak2 inhibition.

Pyrimethamine suppresses cyst formation and growth in *Pkd1* IKO kidneys

We have previously shown that renal IRI accelerates cyst formation in mice with *Pkd1* inactivation induced in adulthood (7). To investigate whether pyrimethamine has a beneficial effect on cystogenesis in this adult PKD mouse model (aIKO), we first immunoblotted pSTAT3 in kidney lysates from aIKO and their littermate wild-type mice at 48 h and 1 week after IRI. Increased STAT3 activation was observed in both wild-type and aIKO injured kidneys at 48 h after IRI when the cell proliferation in the injured kidney reaches a peak (7,31), compared with contralateral (non-ischemic) kidneys (Fig. 4A). One week after IRI, as the kidney recovers, the levels of pSTAT3 in control injured kidneys decreased to a level similar to contralateral (non-ischemic) kidneys. In contrast, pSTAT3 levels failed to decline at 1 week after IRI in aIKO injured kidneys (Fig. 4A), coinciding with the extensive cell proliferation seen in those kidneys (7). Thus, we administered pyrimethamine (25 mg/kg) by gavage to aIKO mice 1 week after bilateral IRI for 4 weeks. It has been reported that a dose of 60 mg/kg, which corresponds to a plasma pyrimethamine concentration of 320 μmol/l (32), achieves a significant reduction in human melanoma growth in a severe combined immunodeficiency mouse model but a lower dose of pyrimethamine (6 mg/kg) does not (33). Therefore, we chose the dose of 25 mg/kg in this study. As expected, neither vehicle- nor drug-treated control injured kidneys developed cysts (Fig. 4Ba and data not shown). Consistent with our previous report (7), multiple cysts were observed in aIKO injured kidneys at 4 weeks after the vehicle treatment (Fig. 4Bb). In contrast, cyst formation was significantly reduced in drug-treated aIKO injured kidneys (Fig. 4Bc). Morphometric analyses revealed that drug-treated aIKO mice have significantly reduced kidney weight, kidney/body weight ratio and cyst number without significant weight loss or other signs of toxicity, compared with vehicle-treated aIKO mice (Fig. 4C and Table 1). To investigate whether pyrimethamine inhibits cell proliferation in aIKO injured kidneys, we injected 5-bromo-2′-deoxyuridine (BrdU) on the 2nd and 3rd days after bilateral IRI to label proliferating cells and stained them 4 weeks later. The intensity of BrdU in *Dolichos biflorus agglutinin* (DBA) positive tubular epithelial cells in drug-treated aIKO injured kidneys and vehicle-treated littermate control injured kidneys were similar, suggesting similar rounds of cell divisions (Fig. 4Bd and f); however, it was much stronger than that in vehicle-treated *Pkd1* aIKO injured kidneys (Fig. 4Be and f). This indicates that the drug-treated *Pkd1* aIKO tubular epithelial cells have regained a normal cellular proliferation response. On the other hand, a dilution of BrdU seen in vehicle-treated aIKO injured kidneys (Fig. 4Be) indicates continuous multiple rounds of cell proliferation, consistent with our previous study (7). Thus, pyrimethamine inhibits cell proliferation in aIKO injured kidneys and subsequently suppresses cyst formation and growth. Moreover, pyrimethamine decreased the expression of pSTAT3 *in vivo* (Fig. 4D). Pyrimethamine appears to reduce the IL-6 expression in drug-treated *Pkd1* aIKO injured kidneys; however, it did not reach statistical significance ($P = 0.051$; Fig. 3E). In summary, pyrimethamine has a beneficial effect on cystogenesis and is an excellent candidate of possible intervention for human ADPKD.

S3I-201 suppresses cyst formation and growth in *Pkd1* IKO kidneys

To further verify the importance of STAT3 signaling in PKD, we administered nIKO mice with a chemical inhibitor of STAT3 activity, S3I-201 (NSC 74859; 10 mg/kg) or vehicle beginning at 3 weeks of age for 5 weeks. S3I-201 is known to inhibit STAT3 homodimer complex formation and STAT3 DNA-binding and transcriptional activities (34). In contrast to the rapid widespread cyst formation in the vehicle-treated group, the S3I-201-treated group displayed no body weight loss but had significantly reduced cystogenesis, shown by significantly reduced kidney weight, kidney/body weight ratio, cyst volume, cyst number and serum creatinine (Fig. 5A and B, Supplementary Material, Fig. S2A and Table 2). Pathological findings seen in H&E-stained kidney

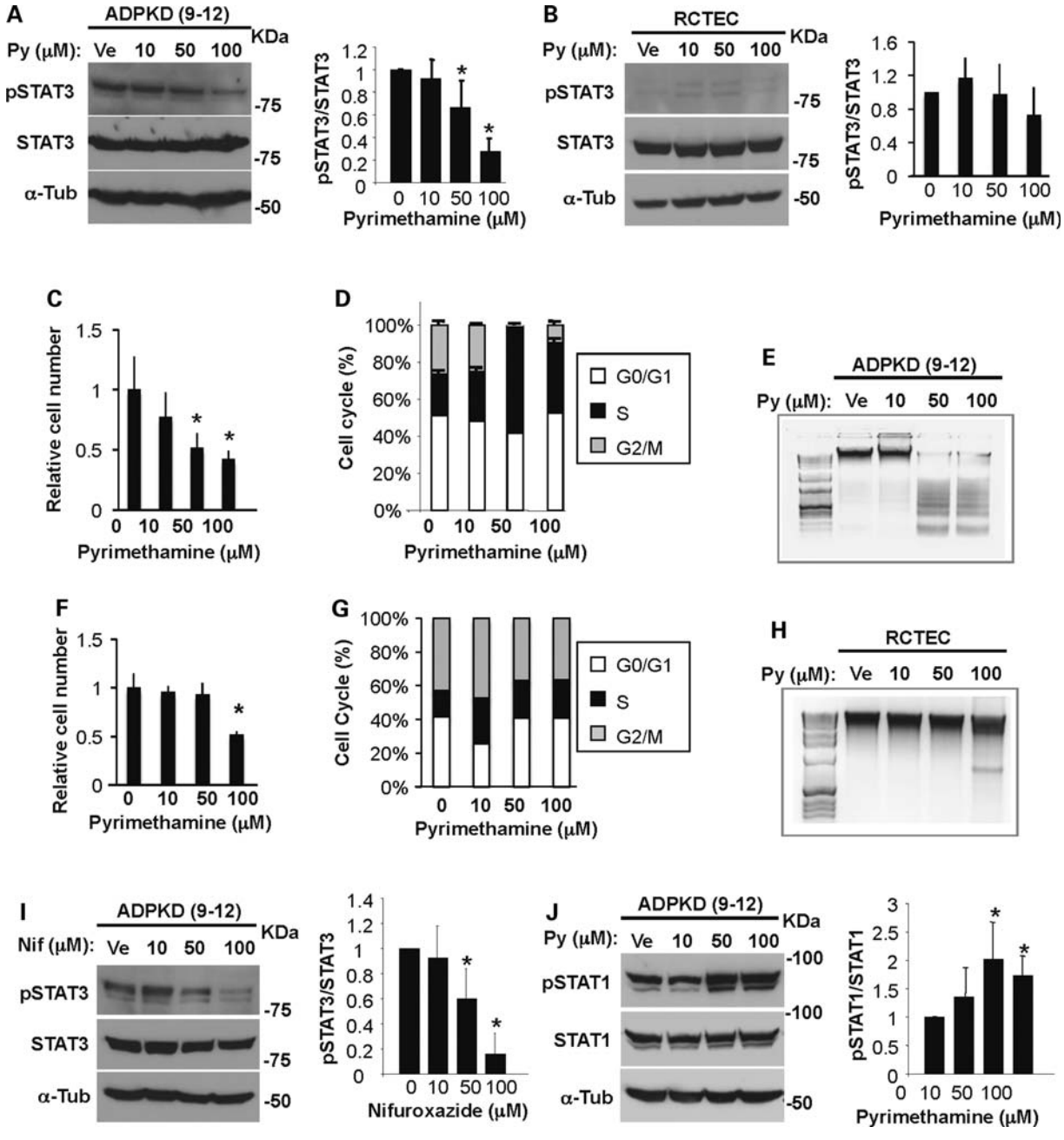

Figure 3. Pyrimethamine inhibits STAT3 tyrosine phosphorylation in human ADPKD cells. Human ADPKD (9–12) cells (**A**) and non-PKD normal epithelial (RCTEC) cells (**B**) were incubated with either vehicle (Ve) or pyrimethamine (Py) at the indicated concentrations for 24 h and were blotted with indicated antibodies. Data shown are representative from three independent experiments. The ratio of pSTAT3/STAT3 band intensity is quantified and shown in the right panel ($^*P < 0.005$). Human ADPKD cells (**C**) and normal cells (**F**) were treated with pyrimethamine as described above. Viable cells excluding Trypan blue were counted ($^*P < 0.05$). Flow-activated cytometry analysis of human ADPKD cells (**D**) and normal cells (**G**) treated with pyrimethamine. Genomic DNA was isolated from human ADPKD cells (**E**) and normal cells (**H**) cultured as in (A) and (B) for 3 days. DNA fragmentation was visualized by 1.2% agarose gel electrophoresis. Human ADPKD cells were incubated with vehicle or nifuroxazide (Nif) (**I**) or pyrimethamine (Py) (**J**) at the indicated concentrations for 24 h followed by blotting with pSTAT3 (I) or STAT1 (J) or total STAT3 (I) or STAT1 (J). α-Tubulin was used as a loading control. The ratio of pSTAT3/STAT3 band intensity is quantified ($^*P < 0.005$). The ratio of pSTAT1/STAT1 band intensity is shown ($^*P < 0.03$). All data shown were expressed as the mean ± SD from three independent experiments. The size of STAT3α, STAT3β, STAT1α, STAT1β and α-tubulin is 79, 86, 84, 91 and 55 kDa, respectively. The protein markers are indicated.

sections of vehicle-treated nIKO kidneys (Fig. 5Ca) including interstitial expansion, multiple small cysts and dilated tubules around large cysts are significantly reduced in S3I-201-treated nIKO kidneys (Fig. 5Cb). Masson's trichrome staining confirms the striking reduction in collagen deposition in S3I-201-treated kidneys, compared with vehicle-treated ones (Fig. 5Cc and d). The improvement in renal histology is accompanied by a reduction in pSTAT3-positive cyst-lining

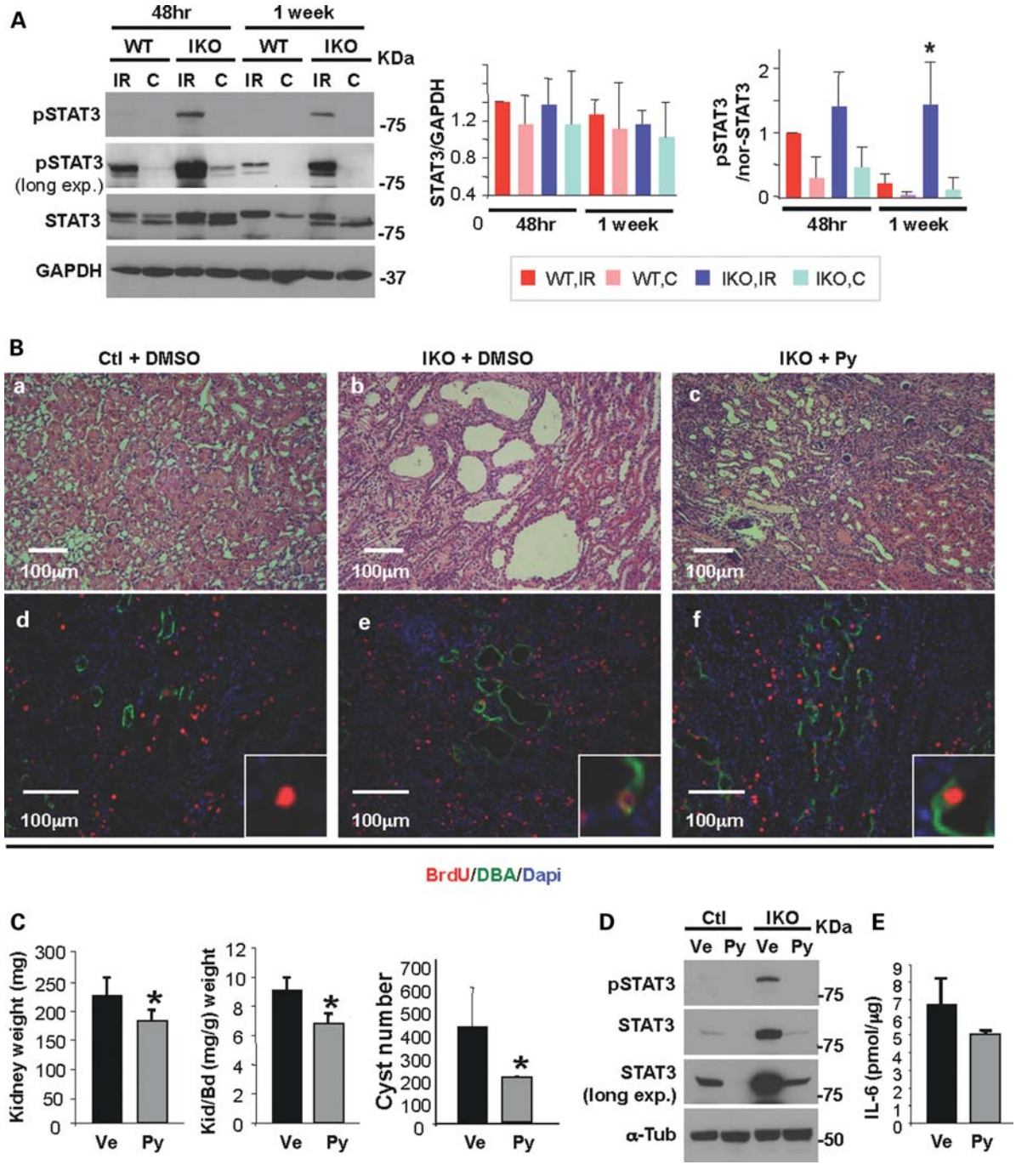

Figure 4. Pyrimethamine suppresses cyst formation and growth in an adult PKD mouse model. (**A**) Unilateral IRI was performed on the *Pkd1* IKO and their littermate wild-type mice, followed by reperfusion for 48 h or 1 week. Western blot analyses of kidney extracts from *Pkd1* IKO (IKO) and control (WT) mice were performed. GAPDH was used as a loading control. IR, injured kidney; C, contralateral (non-ischemic) kidney. Data shown are representative from three mice per group. STAT3 expression is normalized to GAPDH and the ratio of pSTAT3/STAT3 is normalized to the loading control GAPDH [pSTAT3/nor-STAT3, 1 week-WT-IR versus 1 week-IKO-IR, $^{*}P < 0.02$). (**B**) Representative H&E staining of kidney sections are shown in (a–c). Kidney sections were double-labeled with anti-BrdU antibody (red) and DBA (green) (d–f). The *Pkd1* IKO mice shown here are male *Mx1Cre*$^{+}$*Pkd1*$^{flox/flox}$ mice. (**C**) Kidney weight (left, $^{*}P < 0.05$), kidney and body weight ratio (middle, $^{*}P < 0.02$) and cyst number (right, $^{*}P < 0.038$) of vehicle- or pyrimethamine-treated *Pkd1* IKO mice are shown ($n = 4$ mice per group). (**D**) Western blot analyses of kidney extracts from either vehicle- or drug-treated *Pkd1* IKO and control mice show that activated STAT3 decreases in both *Pkd1* IKO and control kidneys with drug treatment. α-Tubulin was used as a loading control. (**E**) IL-6 production in kidney lysates from either vehicle- or drug-treated *Pkd1* IKO mice was measured by enzyme-linked immunosorbent assay ($n = 3$ mice per each genotype). The genotype for the *Pkd1* IKO mice is *Mx1Cre*$^{+}$*Pkd1*$^{flox/flox}$. All data shown here were expressed as the mean ± SD. The size of STAT3α, STAT3β, GAPDH and α-tubulin is 79, 86, 37 and 55 kDa, respectively. The protein markers are indicated.

Table 1. The effect of pyrimethamine in an adult PKD model

	Number of animals	Body weight (g)	Kidney weight (mg)	K/BW ratio (mg/g)	Cyst number
Vehicle	4 (2 m, 2 f)	24.9 ± 1.5	217.6 ± 27.8	8.7 ± 1.0	426 ± 166
Pyrimethamine	4 (2 m, 2 f)	26.2 ± 2.2	177.6 ± 15.1	6.8 ± 0.5	197 ± 4
P-value		NS	$P < 0.023$	$P < 0.007$	$P < 0.038$

m, male; f, female.

epithelial cells and interstitial cells in drug-treated mouse kidneys (Fig. 5D). Moreover, the mRNA expression of STAT3 target genes in S3I-201-treated nIKO kidneys was significantly reduced, compared with vehicle-treated nIKO kidneys, and was similar to un-treated wild-type kidneys (Fig. 5E). S3I-201 is also effective in suppressing STAT3 activation in human ADPKD cells (Fig. 5F). Similar to pyrimethamine-treated ADPKD cells, S3I-201-treated ADPKD cells exhibited reduction in G2/M phase and increase in S phase (Fig. 5G and Supplementary Material, Table S1).

We also treated nIKO mice with pyrimethamine (12.5 mg/kg). As expected, pyrimethamine dramatically reduced cystogenesis (Supplementary Material, Fig. S2A). These data suggest that blocking STAT3 signaling represents a novel approach to reduce cystogenesis in human ADPKD.

DISCUSSION

We have recently proposed the 'third-hit' hypothesis for ADPKD in adult life (3) and demonstrated that renal injury acts as a 'third-hit' and facilitates rapid cyst development in mice with adult inactivation of *Pkd1* (7). Subsequently, Happe *et al*. (35) reported that dichlorovinyl cysteine-induced renal injury also accelerates cyst formation in adult *Pkd1* IKO mice. Consistent with these findings in mice, a recent human study has demonstrated that two renal allograft recipient patients developed polycystic kidney disease in the donor kidney a few months after kidney transplantation, although the donor patient carried a *PKD1* mutation and did not have cysts for 30 years (28). These data suggest that ischemia experienced during the surgery accelerates cyst formation in humans, further supporting the relevance of our adult PKD IKO mouse model to the human condition. In this study, we have tested a possible intervention for ADPKD in both adult and neonatal orthologous mouse models of human ADPKD.

We observed sustained pSTAT3 expression in *Pkd1* IKO injured kidneys 1 week after IRI, when it was decreased in wild-type injured kidneys. It has been reported that cell proliferation peaks 48 h after IRI and reverts to the baseline 1 week later. These data indicate that STAT3 activation may be necessary for injury-induced cell proliferation of surviving tubular cells, yet STAT3 needs to be inactivated to turn off this proliferation when the repair phase is complete. Together, these data suggest that PC1 negatively regulates STAT3 activation, either directly or indirectly. Because the increased STAT3 activation was also found in non-injury-induced mouse cystic kidneys and human ADPKD kidneys, it is likely that STAT3 activation is, at least partially, required for the initiation and maintenance of cyst formation and growth. Interventions targeted to the STAT3 pathway may offer considerable therapeutic benefit for patients with ADPKD.

To accelerate the clinical translation of a STAT3 inhibitor, we screened a library of compounds already known to be safe in humans. We identified pyrimethamine as an inhibitor of STAT3 function. Pyrimethamine inhibits the activating tyrosine phosphorylation of STAT3. However, since it also inhibits STAT3-dependent transcription at doses lower than that needed for the inhibition of STAT3 phosphorylation in cancer cell lines, it likely has additional effects as well. Increasing evidence suggests that STAT1 mediates apoptosis, necrosis and autophagy. STAT3 regulates cell proliferation through modulating cell cycle progression and cell survival through anti-apoptotic signaling. Therefore, pyrimethamine-induced cell death and cell growth arrest may be the combined effects of up-regulation of STAT1 activity and down-regulation of STAT3 activity. Pyrimethamine is known as an inhibitor of the enzyme dihydrofolate reductase (DHFR). Another DHFR inhibitor methotrexate (36) and S3I-201 as well as Jak2 inhibitor AG490 (37) induce S-phase arrest. Therefore, pyrimethamine-induced S-phase arrest may be due to inactivation of either DHFR or STAT3 or both.

Because human ADPKD is usually an adult-onset condition and there is no established treatment for this disease, we utilized an adult-onset PKD mouse model, which is more relevant to the human ADPKD condition than neonatal models, for testing the effectiveness of an FDA-approved drug. To strengthen our data implicating STAT3 signaling as an attractive target for human ADPKD and to exclude the possibility that this beneficial effect is specific to injury accelerated cystic disease, we used an ischemia-independent PKD mouse model and treated with either pyrimethamine, or S3I-201, a STAT3-specific compound that inhibits growth and induces apoptosis preferentially in tumor cells and in obstructive nephropathy (34,38). The effectiveness of S3I-201 and pyrimethamine in reducing cyst formation and growth in non-ischemia injury-induced neonatal PKD mouse model provides further support for STAT3 as a therapeutic target in ADPKD. Since our previous studies (3) did not show any gender difference in the severity of cystic disease in our mouse models, we analyzed both male and female mice to minimize the litter number of lab animals for this study. However, it would be interesting to investigate whether the gender-based differences affect the effectiveness of pyrimethamine and S3I-201 in reducing cystogenesis.

It has been shown that PKD1 overexpression causes STAT1 activation and that activated STAT1 is absent from whole embryo extracts of *Pkd1* null mice (39). However, *Stat1*$^{-/-}$ mice do not have the cystic kidney phenotype (40,41). PC1-mediated STAT1 activation likely has other functions,

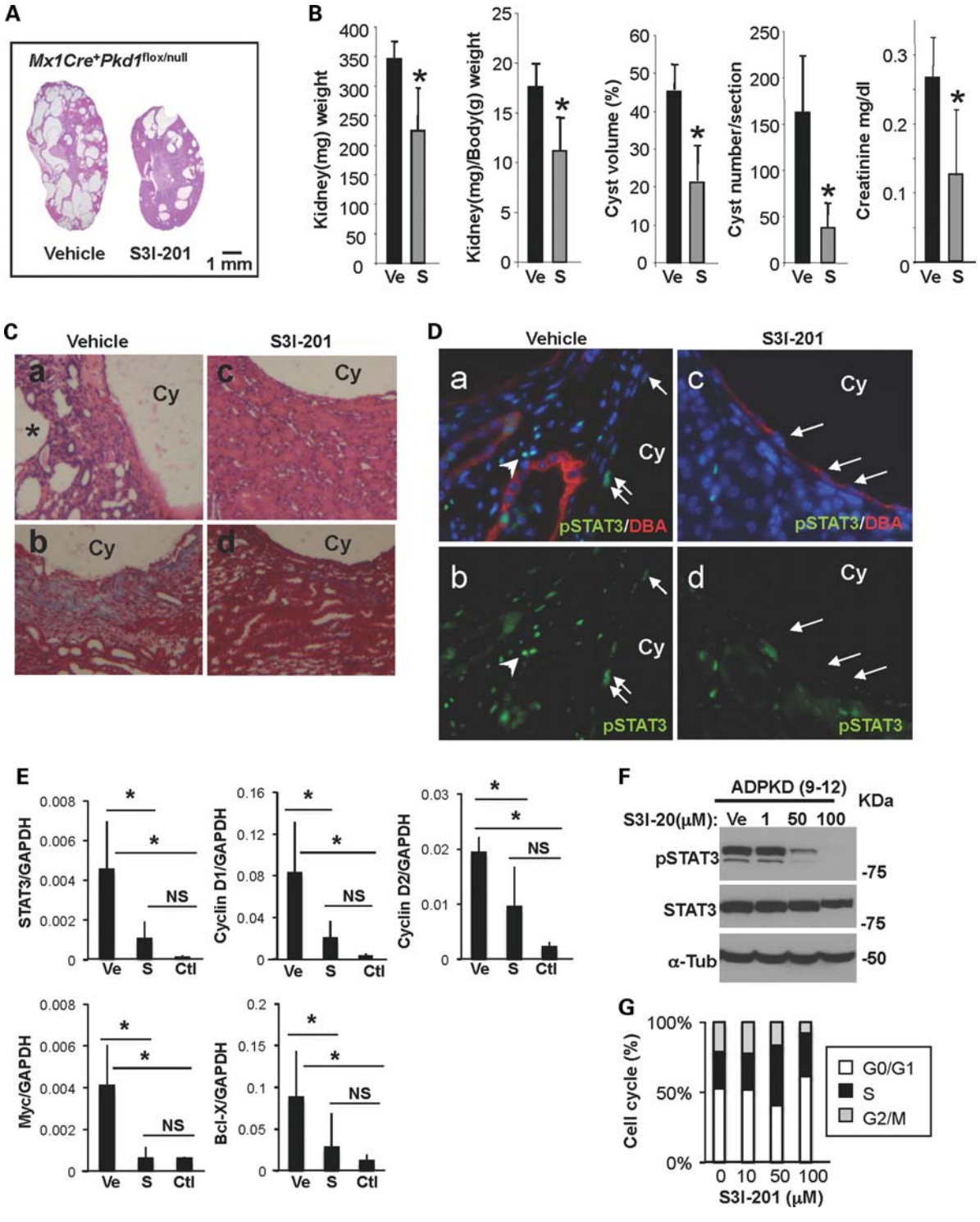

Figure 5. Selective chemical probe inhibitor of STAT3 reduces cyst formation and growth in a neonatal PKD mouse model. (**A**) Representative H&E stained whole kidney sections from vehicle-treated (left) and S3I-201 (right)-treated *Pkd1* IKO (female *Mx1Cre*$^{+}$*Pkd1*$^{flox/null}$) mice. (**B**) Kidney weight ($^{*}P < 0.021$), kidney and body weight ratio ($^{*}P < 0.017$), cyst volume ($^{*}P < 0.019$) and cyst number ($^{*}P < 0.025$) of vehicle- or S3I-201-treated *Pkd1* IKO mice were quantified ($n = 4$ mice per group). Data are expressed as the mean $\pm$ SD. (**C**) Representative H&E (a and c) and Masson's trichrome (b and d) stained kidney sections from vehicle- (a and b) and S3I-201 (c and d)-treated *Pkd1* IKO mice are shown at higher magnification. Collagen deposition is shown in blue. (**D**) Representative immunostaining images of kidney sections from vehicle- (a and b) and S3I-201 (c and d)-treated *Pkd1* IKO mice with pSTAT3 and DBA. Arrows and arrowheads in (a) and (b) point to pSTAT3-positive nuclei of cyst-lining epithelia and interstitial cells, respectively. Arrows in (c) and (d) point to pSTAT3-negative nuclei. Cy represents cyst lumen. (**E**) Real-time RT–PCR was performed on cDNA from vehicle (Ve)- and S3I-201 (S)-treated *Pkd1* IKO kidneys. There was a significant reduction in the expression of STAT3 ($P < 0.02$) and STAT3 target genes c-Myc ($P < 0.008$), cyclin D1 ($P < 0.03$), cyclin D2 ($P < 0.04$) and bcl-X ($P < 0.006$) in S3I-201-treated *Pkd1* IKO kidneys compared with vehicle-treated ones. Un-treated wild-type kidneys (Ctl) were used to show the baseline expression level of the genes of interest. (**F**) Immunoblot of pSTAT3 and total STAT3 in ADPKD cells treated with S3I-201 at the indicated concentrations. (**G**) Flow-activated cytometry analysis of human ADPKD cells treated with either vehicle or S3I-201.

Table 2. The effect of S3I-201 in a neonatal PKD model

	Number of animals	Body weight (g)	Kidney weight (mg)	K/BW ratio (mg/g)	Cyst volume (%)	Cyst number	Serum creatinine (mg/dl)
Vehicle	4 (3 m, 1 f)	21.6 ± 4.5	348.2 ± 23.7	16.5 ± 2.9	42 ± 8	146 ± 59	0.27 ± 0.06
S3I-201	5 (2 m, 3 f)	21.3 ± 3.1	232.5 ± 64.7	10.9 ± 2.9	18 ± 11	34 ± 23	0.13 ± 0.10
P-value		NS	$P < 0.006$	$P < 0.01$	$P < 0.004$	$P < 0.003$	$P < 0.04$

m, male; f, female.

perhaps in bone morphogenesis because both $Pkd1^{-/-}$ and $Stat1^{-/-}$ mice exhibit abnormal skeletal development (42,43). Although PC1 overexpressing cells induce STAT3 activation using a luciferase reporter assay, pSTAT3 was not detectable by western blot.

In summary, our results demonstrate that pyrimethamine and S3I-201 reduce cyst formation and growth *in vivo*. Interventions targeting STAT3, such as the clinically relevant drug pyrimethamine, could be of considerable therapeutic benefit to patients with ADPKD.

MATERIALS AND METHODS

Generation of inducible Pkd1 knockout mice

Inducible *Pkd1* knockout mice were generated by crossing $Pkd1^{flox/+}$ mice with a transgenic mouse line that expresses Cre recombinase under the control of an interferon (IFN)-inducible *Mx1* promoter (*Mx1Cre* mice). The resultant $Mx1Cre^{+}$-$Pkd1^{flox/+}$ mice were bred with either $Pkd1^{flox/+}$ mice or $Pkd1^{null/+}$ mice to generate $Mx1Cre^{+}Pkd1^{flox/flox}$ mice or $Mx1Cre^{+}Pkd1^{null/flox}$ mice, respectively. $Pkd1^{flox/+}$ (*Pkd1* flox heterozygous but without Mx1Cre), $Pkd1^{flox/flox}$ (*Pkd1* flox homozygous but without Mx1Cre) or $Mx1Cre^{+}Pkd1^{+/+}$ (*Pkd1*wild-type but with Mx1Cre*)* mice were used as controls.

Induction of Cre expression

Mice were intraperitoneally injected with 62.5 or 250 μg of the IFN inducer polyinosinic-polycytidylic acid (pI:pC; Sigma-Aldrich, St Louis, MO, USA) for 5 consecutive days at 1 week of age for a neonatal IKO mouse model or 5 weeks of age for an adult IKO mouse model, respectively, to induce the expression of *Cre* recombinase and inactivate *Pkd1*.

Renal IRI model

Studies were performed according to the animal experimental guidelines issued by the Animal Care and Use Committee at Harvard University. The *Pkd1* IKO and their littermate control mice were injected with pI:pC at 5 weeks of age. IRI was performed at 8 weeks of age. Animals were anesthetized with pentobarbital sodium (60 mg/kg body weight, intraperitoneally) prior to surgery. Body temperatures were controlled at 36.5–37.5°C throughout the procedure. Kidneys were exposed through flank incisions, and mice were subjected to ischemia by clamping either only left or both left and right renal pedicle with non-traumatic microaneurysm clamps (Roboz, Rockville, MD, USA), which were removed after 20–25 min (males) or 30–35 min (females). One milliliter of 0.9% NaCl was administered subcutaneously 2 h after surgery. To label proliferating cells, mice were injected with BrdU (Sigma-Aldrich) intraperitoneally (50 mg/kg body weight) on the 2nd and 3rd days after IRI and sacrificed at 4 weeks after treatment.

Preparation and administration of pyrimethamine and S3I-201 in mice

Pyrimethamine (Sigma-Aldrich) was dissolved in 100% dimethyl sulfoxide (DMSO) and administered at 25 mg/kg of body weight by gavage for 5 consecutive days per week until analysis. S3I-201 (EMD4Biosciences, Gibbstown, NJ, USA) was dissolved in 20% DMSO and 80% phosphate-buffered saline (PBS) and administered intraperitoneally at 10 mg/kg of body weight for 5 consecutive days per week until analysis.

Cell culture

Human cell lines from RCTE and ADPKD cyst-lining epithelia (9–12 cell line) were previously immortalized with recombinant ori^{-} adeno-SV40 viruses (44) and were cultured in Dulbecco's modified Eagle's media containing 10% fetal bovine serum.

Generation of reporter cell lines

To identify small molecule inhibitors of STAT3, we performed a cell-based assay quantitatively measuring STAT3-dependent reporter gene expression (30). We used the STAT1 null U3A cell line stably transfected with a STAT3 regulatory element driving luciferase expression. To eliminate non-specific inhibitors and generally cytotoxic compounds, we countered screened using 293 cells containing an NFκB-responsive luciferase gene. We screened the Prestwick Chemical Library, which contains 1120 bioactive compounds. Cells were plated in opaque 384-well plates at a concentration of 2.5×10^3 cells/well and allowed to adhere overnight. Compounds dissolved in DMSO were added to the cells and allowed to incubate for 1 h, after which cytokine was added [10 ng/ml human IL-6 (Peprotech, Rocky Hill, NJ, USA) for STAT3 activation and 10 ng/ml murine tumor necrosis factor-α for NFκB activation]. The final concentration of DMSO was 0.33%. Six hours later, luciferase activity was quantitated using the Bright-Glo Luciferase Assay System from Promega (Madison, WI, USA) and a Luminoskan Ascent luminometer from Labsystems (Helsinki, Finland). Confirmation of activity was determined using the

same assay, except 1×10^4 cells/well were plated in opaque 96-well plates. The final DMSO concentration was 0.1%. To measure the effect of compounds on STAT5 transcriptional activity, a cell line containing a STAT5-responsive luciferase reporter gene was used (30). STAT5 was activated by stimulation with 100 ng/ml of human prolactin (Peptrotech). Pyrimethamine (Sigma-Aldrich) was chosen for further study based on its activity in the STAT3 assay, and the absence of effects in the STAT5 and NFκB assays.

Enzyme-linked immunosorbent assay

Murine IL-6 cytokine was measured in kidney lysates according to the manufacture's instructions (R&D Systems, Minneapolis, MN, USA) and normalized with protein amount.

Histology and immunohistochemistry

Paraffin-embedded sections (4 μm) were dewaxed, rehydrated through graded alcohols and boiled in 10 mM citrate (pH 6.0; VECTOR, Burlingame, CA, USA) for 30 min. The sections were then placed in the staining dish at room temperature and allowed to cool for 1 h. Sections were incubated with 10% goat serum for 30 min and incubated with either anti-tyrosine pSTAT3 antibody (1:200; Cell Signaling, Danvers, MA, USA) or anti-BrdU antibody (1:100; BD Biosciences, San Jose, CA, USA) for 1 h at room temperature. After washing with PBS, sections were incubated with secondary antibody for 1 h at room temperature. For double staining with the tubule marker Lectin DBA (VECTOR), a dilution of 1:500 was used. After washing with PBS, sections were mounted with Prolong Gold antifade reagent with 4′-6-diamidino-2-phenylindole (Invitrogen, Carlsbad, CA, USA).

Western blotting

Kidneys were homogenized with T-PER (Thermo Scientific, Rockford, IL, USA) containing protease inhibitors (Roche, South San Francisco, CA, USA) on ice. Tissue lysates were cleared by centrifugation. Cells were lysed in radio-immunoprecipitation assay buffer (Thermo Scientific) containing protease inhibitors (Roche), and cell lysates were cleared by centrifugation. Equal amounts of lysates (100 μg) were separated on 10 or 12% SDS–PAGE. The proteins were transferred onto nitrocellulose membranes (Amersham, Woburn, MA, USA). The membranes were then blocked with 5% non-fat dry milk in PBS for 30 min incubated overnight at 4°C with antibody to tyrosine pSTAT3 (1:1000; Cell Signaling), STAT3 (1:200; Santa Cruz Biotechnology, Inc., Santa Cruz, CA, USA) or α-tubulin (1:5000; Abcam, Cambridge, MA, USA). After three washings with PBS, the membranes were incubated with peroxidase-conjugated goat anti-mouse immunoglobulin G (IgG) or anti-rabbit IgG (1:5000; Amersham) for 1 h. Finally, the blots were developed by the enhanced chemiluminescence method. Membranes were then stripped of antibodies using RestoreTM Western Blot Stripping Buffer (Thermo Scientific) for 30 min at 37°C. Membranes were then reprobed with primary antibody and secondary antibodies.

Cell cycle analysis

Human ADPKD cells were treated with pyrimethamine at the indicated concentration for 24 h. Cells were then fixed with 70% ethanol and stored at 4°C until flow cytometry analysis. Fixed cells were stained with 50 μg/ml of propidium iodide solution containing 10 mM Tris, pH 7.5, 5 mM $MgCl_2$ and 10 μg/ml of RNase A (guaranteed DNase free).

Measurement of cyst volume

The cyst volume was quantified in whole-kidney H&E staining sections using Image Pro Plus v5 software (Media Cybernetics) and calculated as (cystic area/total kidney area) × 100%. Two sections from both kidneys were analyzed for each mouse.

Real-time RT–PCR

Real-time RT–PCR was performed using the following primers sets: β-actin forward 5′-GCA CAG CTT CTT TGC AGC TC-3′, β-actin reverse 5′-GCA GCG ATA TCG TCA TCC AT-3′, GAPDH forward 5′-CAA GAT TGT CAG CAA TGC ATC C-3′, GAPDH reverse 5′-TGG CAG TGA TGG CAT GGA CT-3′, Cyclin D1 forward 5′-TGA AGG AGA CCA TTC CCT TG-3′, Cyclin D1 reverse 5′- CCA CTT GAG CTT GTT CAC CA-3′, Cyclin D2 forward 5′-CAT CTG TGG GCT TCA GCA G-3′, Cyclin D2 reverse 5′-ATG CTG CTC TTG ACG GAA CT-3′, c-Myc forward 5′-CTG CTG TCC TCC GAG TCC T-3′, c-Myc reverse 5′-GAT GGA GAT GAG CCC GAC T-3′, Bcl-X forward 5′-GGT GAG TCG GAT TGC AAG TT-3′ and Bcl-X reverse 5′-TGT TCC CGT AGA GAT CCA CA-3′.

Statistic analysis

The significance of differences between groups was determined by Student's *t*-test. A *P*-value of <0.05 was considered statistically significant.

SUPPLEMENTARY MATERIAL

Supplementary Material is available at *HMG* online.

ACKNOWLEDGEMENTS

The authors would like to thank Ms C LaPierre for excellent technical assistance and other members of Zhou Lab and the Harvard Center of Polycystic Kidney Disease Research for scientific discussions and support.

Conflict of Interest statement. None declared.

FUNDING

This work was supported by grants from the National Institutes of Health (DK51050 and DK40703) to J.Z. and DK074030 to the Harvard Center of Polycystic Kidney Disease (J.Z. and A.T.) and Scientist Development Grant from American Heart Association to A.T.

REFERENCES

1. Gabow, P.A. (1993) Autosomal dominant polycystic kidney disease. *N. Engl. J. Med.*, **329**, 332–342.
2. Peters, D.J. and Sandkuijl, L.A. (1992) Genetic heterogeneity of polycystic kidney disease in Europe. *Contrib. Nephrol.*, **97**, 128–139.
3. Takakura, A., Contrino, L., Beck, A.W. and Zhou, J. (2008) Pkd1 inactivation induced in adulthood produces focal cystic disease. *J. Am. Soc. Nephrol.*, **19**, 2351–2363.
4. Piontek, K., Menezes, L.F., Garcia-Gonzalez, M.A., Huso, D.L. and Germino, G.G. (2007) A critical developmental switch defines the kinetics of kidney cyst formation after loss of Pkd1. *Nat. Med.*, **13**, 1490–1495.
5. Lantinga-van Leeuwen, I.S., Leonhard, W.N., van der Wal, A., Breuning, M.H., de Heer, E. and Peters, D.J. (2007) Kidney-specific inactivation of the Pkd1 gene induces rapid cyst formation in developing kidneys and a slow onset of disease in adult mice. *Hum. Mol. Genet.*, **16**, 3188–3196.
6. Bonventre, J.V. (2003) Dedifferentiation and proliferation of surviving epithelial cells in acute renal failure. *J. Am. Soc. Nephrol.*, **14** (Suppl. 1), S55–S61.
7. Takakura, A., Contrino, L., Zhou, X., Bonventre, J.V., Sun, Y., Humphreys, B.D. and Zhou, J. (2009) Renal injury is a third hit promoting rapid development of adult polycystic kidney disease. *Hum. Mol. Genet.*, **18**, 2523–2531.
8. Ghatpande, S., Goswami, S., Mascareno, E. and Siddiqui, M.A. (1999) Signal transduction and transcriptional adaptation in embryonic heart development and during myocardial hypertrophy. *Mol. Cell. Biochem.*, **196**, 93–97.
9. Mascareno, E., El-Shafei, M., Maulik, N., Sato, M., Guo, Y., Das, D.K. and Siddiqui, M.A. (2001) JAK/STAT signaling is associated with cardiac dysfunction during ischemia and reperfusion. *Circulation*, **104**, 325–329.
10. Johansen, K.A., Iwaki, D.D. and Lengyel, J.A. (2003) Localized JAK/STAT signaling is required for oriented cell rearrangement in a tubular epithelium. *Development*, **130**, 135–145.
11. Pires-daSilva, A. and Sommer, R.J. (2003) The evolution of signalling pathways in animal development. *Nat. Rev. Genet.*, **4**, 39–49.
12. Xi, R., McGregor, J.R. and Harrison, D.A. (2003) A gradient of JAK pathway activity patterns the anterior-posterior axis of the follicular epithelium. *Dev. Cell*, **4**, 167–177.
13. Aaronson, D.S. and Horvath, C.M. (2002) A road map for those who don't know JAK-STAT. *Science*, **296**, 1653–1655.
14. Zhang, Y.W., Wang, L.M., Jove, R. and Vande Woude, G.F. (2002) Requirement of Stat3 signaling for HGF/SF-Met mediated tumorigenesis. *Oncogene*, **21**, 217–226.
15. Grantham, J.J. (1997) Mechanisms of progression in autosomal dominant polycystic kidney disease. *Kidney Int. Suppl.*, **63**, S93–S97.
16. Merta, M., Tesar, V., Zima, T., Jirsa, M., Rysava, R. and Zabka, J. (1997) Inflammatory cytokine profile in autosomal dominant polycystic kidney disease. *Contrib. Nephrol.*, **122**, 35–37.
17. Qin, S., Taglienti, M., Nauli, S.M., Contrino, L., Takakura, A., Zhou, J. and Kreidberg, J.A. (2010) Failure to ubiquitinate c-Met leads to hyperactivation of mTOR signaling in a mouse model of autosomal dominant polycystic kidney disease. *J. Clin. Invest.*, **120**, 3617–3628.
18. Yokogami, K., Wakisaka, S., Avruch, J. and Reeves, S.A. (2000) Serine phosphorylation and maximal activation of STAT3 during CNTF signaling is mediated by the rapamycin target mTOR. *Curr. Biol.*, **10**, 47–50.
19. Shillingford, J.M., Murcia, N.S., Larson, C.H., Low, S.H., Hedgepeth, R., Brown, N., Flask, C.A., Novick, A.C., Goldfarb, D.A., Kramer-Zucker, A. *et al.* (2006) The mTOR pathway is regulated by polycystin-1, and its inhibition reverses renal cystogenesis in polycystic kidney disease. *Proc. Natl Acad. Sci. USA*, **103**, 5466–5471.
20. Lieberthal, W., Fuhro, R., Andry, C.C., Rennke, H., Abernathy, V.E., Koh, J.S., Valeri, R. and Levine, J.S. (2001) Rapamycin impairs recovery from acute renal failure: role of cell-cycle arrest and apoptosis of tubular cells. *Am. J. Physiol. Renal. Physiol.*, **281**, F693–F706.
21. Masuda, M., Suzui, M., Yasumatu, R., Nakashima, T., Kuratomi, Y., Azuma, K., Tomita, K., Komiyama, S. and Weinstein, I.B. (2002) Constitutive activation of signal transducers and activators of transcription 3 correlates with cyclin D1 overexpression and may provide a novel prognostic marker in head and neck squamous cell carcinoma. *Cancer Res.*, **62**, 3351–3355.
22. Horiguchi, A., Oya, M., Shimada, T., Uchida, A., Marumo, K. and Murai, M. (2002) Activation of signal transducer and activator of transcription 3 in renal cell carcinoma: a study of incidence and its association with pathological features and clinical outcome. *J. Urol.*, **168**, 762–765.
23. Luan, F.L., Hojo, M., Maluccio, M., Yamaji, K. and Suthanthiran, M. (2002) Rapamycin blocks tumor progression: unlinking immunosuppression from antitumor efficacy. *Transplantation*, **73**, 1565–1572.
24. Leonhard, W.N., van der Wal, A., Novalic, Z., Kunnen, S.J., Gansevoort, R.T., Breuning, M.H., de Heer, E. and Peters, D.J. (2011) Curcumin inhibits cystogenesis by simultaneous interference of multiple signaling pathways: *in vivo* evidence from a Pkd1-deletion model. *Am. J. Physiol. Renal Physiol.*, **300**, 1193–1202.
25. Kolpakova-Hart, E., Nicolae, C., Zhou, J. and Olsen, B.R. (2008) Col2-Cre recombinase is co-expressed with endogenous type II collagen in embryonic renal epithelium and drives development of polycystic kidney disease following inactivation of ciliary genes. *Matrix Biol.*, **27**, 505–512.
26. Walz, G., Budde, K., Mannaa, M., Nurnberger, J., Wanner, C., Sommerer, C., Kunzendorf, U., Banas, B., Horl, W.H., Obermuller, N. *et al.* (2010) Everolimus in patients with autosomal dominant polycystic kidney disease. *N. Engl. J. Med.*, **363**, 830–840.
27. Serra, A.L., Poster, D., Kistler, A.D., Krauer, F., Raina, S., Young, J., Rentsch, K.M., Spanaus, K.S., Senn, O., Kristanto, P. *et al.* (2010) Sirolimus and kidney growth in autosomal dominant polycystic kidney disease. *N. Engl. J. Med.*, **363**, 820–829.
28. Canaud, G., Knebelmann, B., Harris, P.C., Vrtovsnik, F., Correas, J.M., Pallet, N., Heyer, C.M., Letavernier, E., Bienaime, F., Thervet, E. *et al.* (2010) Therapeutic mTOR inhibition in autosomal dominant polycystic kidney disease: what is the appropriate serum level? *Am. J. Transplant.*, **10**, 1701–1706.
29. Torres, V.E., Boletta, A., Chapman, A., Gattone, V., Pei, Y., Qian, Q., Wallace, D.P., Weimbs, T. and Wuthrich, R.P. (2010) Prospects for mTOR inhibitor use in patients with polycystic kidney disease and hamartomatous diseases. *Clin. J. Am. Soc. Nephrol.*, **5**, 1312–1329.
30. Nelson, E.A., Walker, S.R., Kepich, A., Gashin, L.B., Hideshima, T., Ikeda, H., Chauhan, D., Anderson, K.C. and Frank, D.A. (2008) Nifuroxazide inhibits survival of multiple myeloma cells by directly inhibiting STAT3. *Blood*, **112**, 5095–5102.
31. Humphreys, B.D., Valerius, M.T., Kobayashi, A., Mugford, J.W., Soeung, S., Duffield, J.S., McMahon, A.P. and Bonventre, J.V. (2008) Intrinsic epithelial cells repair the kidney after injury. *Cell Stem Cell*, **2**, 284–291.
32. Klinker, H., Langmann, P. and Richter, E. (1996) Plasma pyrimethamine concentrations during long-term treatment for cerebral toxoplasmosis in patients with AIDS. *Antimicrob. Agents Chemother.*, **40**, 1623–1627.
33. Giammarioli, A.M., Maselli, A., Casagrande, A., Gambardella, L., Gallina, A., Spada, M., Giovannetti, A., Proietti, E., Malorni, W. and Pierdominici, M. (2008) Pyrimethamine induces apoptosis of melanoma cells via a caspase and cathepsin double-edged mechanism. *Cancer Res.*, **68**, 5291–5300.
34. Siddiquee, K., Zhang, S., Guida, W.C., Blaskovich, M.A., Greedy, B., Lawrence, H.R., Yip, M.L., Jove, R., McLaughlin, M.M., Lawrence, N.J. *et al.* (2007) Selective chemical probe inhibitor of Stat3, identified through structure-based virtual screening, induces antitumor activity. *Proc. Natl Acad. Sci. USA*, **104**, 7391–7396.
35. Happe, H., Leonhard, W.N., van der Wal, A., van de Water, B., Lantinga-van Leeuwen, I.S., Breuning, M.H., de Heer, E. and Peters, D.J. (2009) Toxic tubular injury in kidneys from Pkd1-deletion mice accelerates cystogenesis accompanied by dysregulated planar cell polarity and canonical Wnt signaling pathways. *Hum. Mol. Genet.*, **18**, 2532–2542.
36. Oguariri, R.M., Adelsberger, J.W., Baseler, M.W. and Imamichi, T. (2010) Evaluation of the effect of pyrimethamine, an anti-malarial drug, on HIV-1 replication. *Virus Res.*, **153**, 269–276.
37. Fuke, H., Shiraki, K., Sugimoto, K., Tanaka, J., Beppu, T., Yoneda, K., Yamamoto, N., Ito, K., Masuya, M. and Takei, Y. (2007) Jak inhibitor induces S phase cell-cycle arrest and augments TRAIL-induced apoptosis in human hepatocellular carcinoma cells. *Biochem. Biophys. Res. Commun.*, **363**, 738–744.
38. Pang, M., Ma, L., Gong, R., Tolbert, E., Mao, H., Ponnusamy, M., Chin, Y.E., Yan, H., Dworkin, L.D. and Zhuang, S. (2010) A novel STAT3 inhibitor, S3I-201, attenuates renal interstitial fibroblast activation and interstitial fibrosis in obstructive nephropathy. *Kidney Int.*, **78**, 257–268.
39. Bhunia, A.K., Piontek, K., Boletta, A., Liu, L., Qian, F., Xu, P.N., Germino, F.J. and Germino, G.G. (2002) PKD1 induces p21(waf1) and

regulation of the cell cycle via direct activation of the JAK-STAT signaling pathway in a process requiring PKD2. *Cell*, **109**, 157–168.
40. Durbin, J.E., Hackenmiller, R., Simon, M.C. and Levy, D.E. (1996) Targeted disruption of the mouse Stat1 gene results in compromised innate immunity to viral disease. *Cell*, **84**, 443–450.
41. Meraz, M.A., White, J.M., Sheehan, K.C., Bach, E.A., Rodig, S.J., Dighe, A.S., Kaplan, D.H., Riley, J.K., Greenlund, A.C., Campbell, D. *et al.* (1996) Targeted disruption of the Stat1 gene in mice reveals unexpected physiologic specificity in the JAK-STAT signaling pathway. *Cell*, **84**, 431–442.
42. Sahni, M., Ambrosetti, D.C., Mansukhani, A., Gertner, R., Levy, D. and Basilico, C. (1999) FGF signaling inhibits chondrocyte proliferation and regulates bone development through the STAT-1 pathway. *Genes Dev.*, **13**, 1361–1366.
43. Lu, W., Shen, X., Pavlova, A., Lakkis, M., Ward, C.J., Pritchard, L., Harris, P.C., Genest, D.R., Perez-Atayde, A.R. and Zhou, J. (2001) Comparison of Pkd1-targeted mutants reveals that loss of polycystin-1 causes cystogenesis and bone defects. *Hum. Mol. Genet.*, **10**, 2385–2396.
44. Nauli, S.M., Rossetti, S., Kolb, R.J., Alenghat, F.J., Consugar, M.B., Harris, P.C., Ingber, D.E., Loghman-Adham, M. and Zhou, J. (2006) Loss of polycystin-1 in human cyst-lining epithelia leads to ciliary dysfunction. *J. Am. Soc. Nephrol.*, **17**, 1015–1025.